PHYSICAL REVIEW C VOLUME 22, NUMBER 4 OCTOBER 1980

Thermodynamic properties of hot nucleonic matter

Manuel Barranco
Department of Physics, University of Florida, Gainesville, Florida 32611
and Institut de Physique Nucléaire, Division de Physique Théorique, 91406 Orsay, France

J. Robert Buchler
Departments of Physics and of Astronomy, University of Florida, Gainesville, Florida 32611
(Received 3 March 1980)

Phase diagrams for bulk nuclear matter at finite temperatures and variable proton concentrations are presented and discussed. This binary system exhibits a line of critical points, a line of equal concentrations, and a line of maximum temperatures. the phenomenon of retrograde condensation is also possible.

[NUCLEAR STRUCTURE Phase diagrams of nuclear matter, equation of state.]

I. INTRODUCTION

The study of hot, dense matter has important astrophysical applications. Supernova models involve the gravitational collapse of the inner core of a massive star followed by the explosive ejection of the overlying material. This collapse brings matter beyond nuclear matter density ($\rho_{NM} \sim 2.7 \times 10^{14}$ g/cm^3) and to temperatures in excess of 10 MeV. At several times nuclear matter density both the dominance of the yet nonrelativistic nucleons over the extreme-relativistic electrons and short-range nuclear repulsion cause an abrupt stiffening of the equation of state (EOS). This gives rise to a bounce of the collapsing core and to the formation of an outward moving shockwave. During the collapse electron captures create copious amounts of neutrinos and neutronize matter. Since the original suggestion by Colgate and White[1] the hope has been that these neutrinos will exert enough stress on the infalling material to reinforce the shockwave and produce a strong explosion. Recent spherically symmetric hydrodynamic model calculations of the collapse[2,3] have thwarted that hope; the neutrinos are not released sufficiently fast and, if anything, tend to weaken the shock, so that explosions are marginal at best. These calculations have shown that the outcome of the collapse is very sensitive to the equation of state from subnuclear to supernuclear densities. Recent two-dimensional numerical hydrodynamic calculations[4] indicate that an expected Rayleigh-Taylor[5,6] instability gives rise to a large-scale, violent overturn of the core and results in a strong explosion.[7] The formation of such a crucial Rayleigh-Taylor unstable region during the bounce of the core, however, depends sensitively on the equation of state at subnuclear density.

At subnuclear densities matter is composed of nuclei, free nucleons, leptons, and photons.[8-13] It is known[10] that the gross features of the equation of state are determined by the bulk properties of matter: Surface and Coulomb effects basically determine details such as the sizes of nuclei. This then lends more than just academic interest to the study of bulk matter. When using the equation of state of bulk matter as a first approximation to the actual equation of state, it is crucial to consider the possibility of phase coexistence as will be shown (especially Figs. 2 and 3).

Bulk properties of homogeneous matter at finite temperatures have received a fair amount of recent interest.[13-19] However, only two works[9,13] also discuss the stability of hot nucleonic matter and the possibility of coexistence of several phases. One of these,[19] however, has overlooked some interesting and unexpected properties of such matter which will be discussed in the present paper.

II. HOMOGENEOUS MATTER

Our free-energy density functional f has the form

$$f(\rho, Y, T) = f_{NI}(\rho, Y, T) + v(\rho, Y), \tag{1}$$

where the noninteracting part, f_{NI}, is given as the sum of separate proton and neutron contributions, $f_0(\rho_p, T)$ and $f_0(\rho_n, T)$, with respective number densities $\rho_p = Y\rho$ and $\rho_n = (1 - Y)\rho$, where Y is thus the proton concentration. The functions $f_0(\rho, T)$ are obtained numerically from the functional fits to the grand potential Ω (or pressure, p) and density ρ (see appendix of the second Ref. 15). The functional form of the interaction energy density $v(\rho, Y)$ is the same as in Buchler and Epstein[20] and is exhibited in Fig. 1. It corresponds to an interpolation between the variable Y functional fit of Lombard[21] (the coefficients in that reference con-

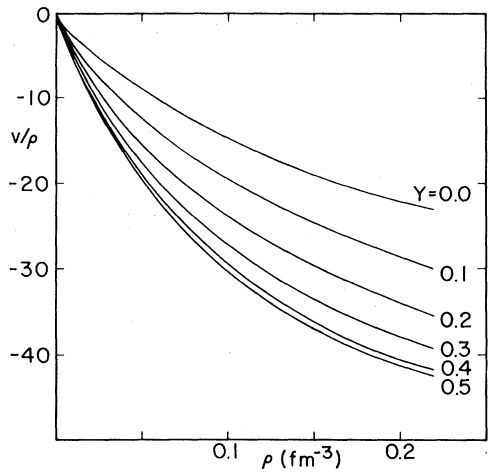

FIG. 1. Nuclear interaction energy per nucleon as a function of nucleon density for various values of proton concentration, Y.

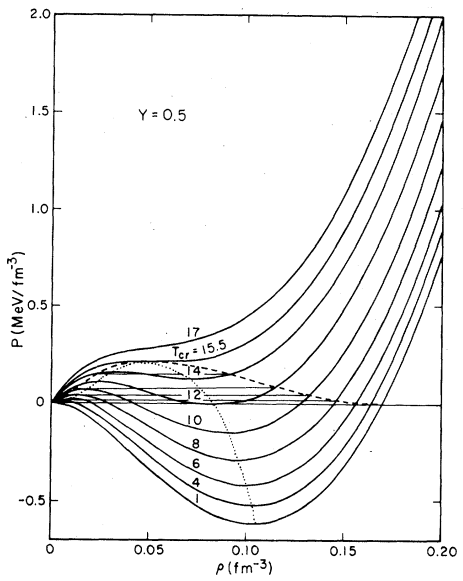

FIG. 2. Pressure-density isotherms for a single phase with $Y = 0.5$. The region where the stability criteria (3–5) are violated is bounded by the dotted line. The dashed line denotes the phase-separation boundary. The horizontal line shows the actual behavior of the equation state.

tain misprints and should read $b_1 = -818.25$, $b_2 = 1371.06$, $b_3 = -556.55$, $a_1 = -0.316$, $a_2 = 0.2$, $a_3 = 1.646$) and the pure neutron gas calculation of Buchler and Ingber.[22]

The interaction energy $v(\rho, Y)$ is assumed to be temperature independent, mostly for lack of better knowledge. *Ab initio* finite temperature many-body calculations using the Bloch-DeDominicis formalism exist only for a pure neutron gas at subnuclear densities.[15] The existing finite temperature Hartree-Fock calculations,[14,16,19] on the other hand, use a temperature *independent* model effective interaction; such an approach has been shown[17] to be valid only at low temperature since it is based on a high degeneracy approximation. We thus believe our energy functional to be adequate given the present state of the art. In any case the results described in this paper have been found to be qualitatively insensitive to the exact form of v.

Nucleonic matter is not thermodynamically stable at all densities, temperatures, and proton concentrations, Y. Necessary and sufficient conditions for stability, $\Delta G \geq 0$, for a binary system (e.g., Ref. 23) can be expressed by the following set of inequalities:

$$C_v \equiv \left(\frac{\partial u}{\partial T}\right)_{\rho Y} > 0 , \tag{3}$$

$$\kappa \equiv \left(\frac{\partial p}{\partial \rho}\right)_{TY} \geq 0 , \tag{4}$$

$$\left(\frac{\partial \mu_n}{\partial Y}\right)_{pT} \leq 0 \text{ or } \left(\frac{\partial \mu_p}{\partial Y}\right)_{pT} \geq 0 . \tag{5}$$

In addition, of course, the pressure, p, must be positive. A positive specific heat, C_v, guarantees thermodynamic stability, a positive compressibility, κ, guarantees mechanical stability, and the condition on the variation of the chemical potentials guarantees diffusive stability. The specific heat is always positive for our energy functional, but the compressibility κ can be negative at large Y and low temperature as one sees upon inspecting isotherms, e.g., for symmetric ($Y = 0.5$) nucleonic matter shown in Fig. 2. The downward sloping parts of the curves, bounded by the dotted line, are obviously unstable. The isotherm with a horizontal inflexion point corresponds to the *critical temperature*. Another unstable region occurs where the pressure is negative; under such conditions the system collapses until a state with $p = 0$ (stable self-bound) is attained. Equilibrium densities as a function of temperature can thus be read off Fig. 2.

For sufficiently small proton concentrations, e.g., for $Y = 0.1$, as shown in Fig. 3, there no longer exists a region of negative pressures, nor even of negative compressibility, at any temperature; this is a consequence of the reduced nuclear symmetry energy. Now, however, the diffusive stability criterion is violated in some regions (dotted lines). In general, for a given Y, criterion (4) or (5) may be violated.

The diffusively unstable regions can be seen more clearly in chemical potential isobars (Fig. 4); according to inequality (5), the region of negative (positive) slope for μ_p (μ_n) is unstable. In order to facilitate a comparison with previous

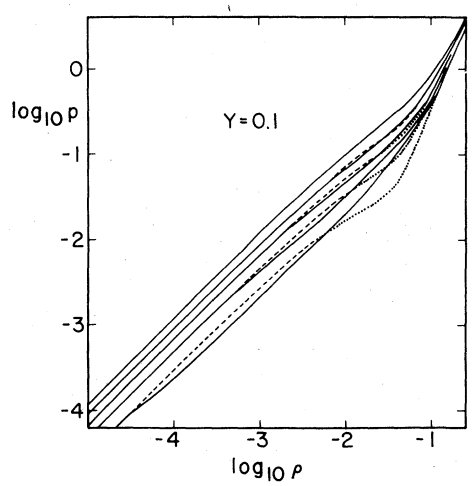

Fig. 3. Pressure-density isotherms for $Y=0.1$. The solid curve represents the actual equation of state. The dashed line denotes the metastable part of the single phase and the dotted line the unstable single phase. The isotherms go from 3, 5, 7, 9, to 12 MeV (pressures in MeV/fm^3, densities in fm^{-3}). All logarithms in this and subsequent figures are base ten.

work[19] we have chosen the same physical parameters and notation. The overall structure of these isobars is very similar to theirs, although the temperature dependence is noticeably different, especially towards the high temperatures (10–20 MeV).

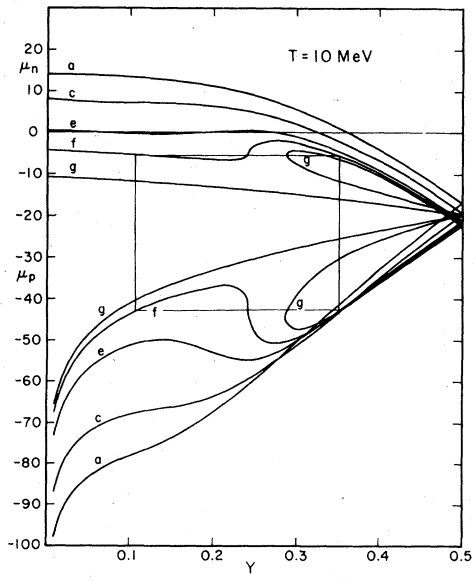

FIG. 4. Neutron and proton chemical potential isobars. The labels refer to the pressures $a=0.88$, $c=0.458$, $e=0.198$, $f=0.115$, and $g=0.058$ MeV/fm^3. The rectangle illustrates the graphical solution of the coexistence equation.

III. TWO PHASE COEXISTENCE

Violation of the stability criteria is indicative of phase separation; the system has no alternative but to split into separate phases in equilibrium. Instability, however, is only a sufficient condition and phase separation may occur even when the one phase system is stable, in general metastable.

In this section we analyze the properties of bulk nuclear matter under those conditions where two distinct phases can coexist. In contrast to the more common single component phase equilibria, such as liquid vapor, in which the phases are distinguished by only one parameter, e.g., the density, in this binary mixture we have, in addition, the proton concentration, Y, which is different from one phase to the other.

We label with subscripts a and b the two coexisting phases and denote the specified *average* density and proton concentration by ρ and Y, respectively. For two phases to coexist at a given temperature, the following well-known[23,24] conditions must be satisfied ($\Delta G=0$):

$$p(\rho_a, Y_a, T)=p(\rho_b, Y_b, T)\,, \tag{6}$$

$$\mu_n(\rho_a, Y_a, T)=\mu_n(\rho_b, Y_b, T)\,, \tag{7}$$

$$\mu_p(\rho_a, Y_a, T)=\mu_p(\rho_b, Y_b, T)\,. \tag{8}$$

It is convenient and customary[23,24] to discuss the phase coexistence in (p, T, Y) space. Because of the assumed isobaric charge symmetry of nuclear forces, the behavior of the system is invariant under a change of Y into $1-Y$ and the phase diagrams are symmetric with respect to $Y=0.5$. We can therefore limit ourselves to the physically more useful neutron-rich region, $Y\in(0, 0.5)$ and in order to avoid crowding of the figures, we occasionally use $\log_{10}Y$ instead of Y.

The phase separation boundary, which encloses all the points for which the two-phase configuration has a lower free energy than the single phase, has the shape of a filet mignon (FM). We have represented it *schematically* in Fig. 5 as an aid to visualize the upcoming discussion associated with Figs. 6 to 8, which are accurate. This FM is itself composed of two subregions, a metastable region and a labile region, separated by the *instability boundary*, which limits the region inside which at least one of the conditions (3) to (5) is violated. *Critical points* on the FM are defined as having both the same densities and the same proton concentrations. According to Gibbs's phase rule the critical points, if they exist, must lie on a line on the FM, the *line of critical points* (LCP).

The solution to the phase-equilibrium relations (3) to (5) can be obtained graphically, as indicated in Ref. 19, with chemical potential isobars. The solutions must lie at the corners of a rectangle

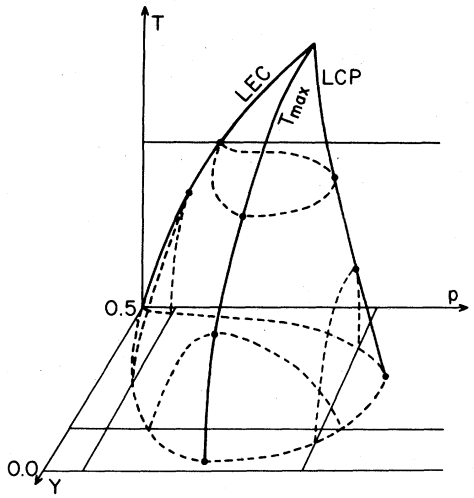

FIG. 5. Schematic representation of the phase-coexistence boundary surface in (p, T, Y) space. Special lines are the line of equal concentration, LEC, the line of critical points, LCP, and the line of maximum temperature, T_{max}.

constructed on the same isobar, as indicated in Fig. 4, which represents isobars at 10 MeV. The instability surface has the well-known property[23] of being tangent to the FM along the LCP (and only there). This can readily be seen from an inspection of the behavior of intersection of a μ_n or μ_p = constant line with various isobars. Isobar (c), e.g., gives rise to only one point of intersection, whereas isobar (e) is cut three times, the central point being inside the unstable region. There exists an intermediate isobar of pressure point, $p \simeq 0.33$ MeV/fm^3, for which the three intersection

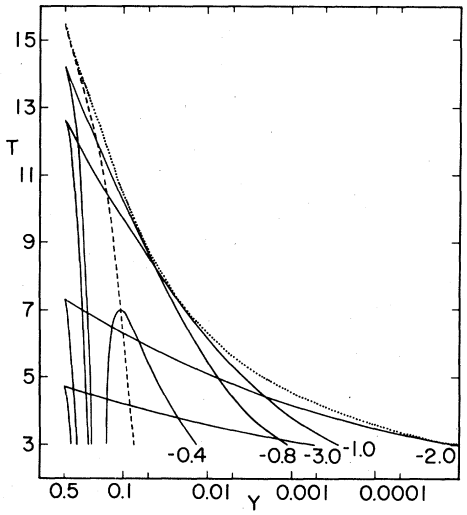

FIG. 7. Cuts of the phase-separation boundary surface orthogonal to p. We show a critical isobar with $\log_{10}p = -0.4$. All the other corresponds to equal-concentration isobars. The dashed line is the projection of the critical line, the dotted line the projection of the maximum temperature line.

points meet (horizontal inflexion point) and which is therefore both a critical point and an unstable point.

Figure 6 represents FM cuts, orthogonal to the T axis, for various values of T. One can see that for each temperature $T < T^* \equiv 15.5$ MeV, there exists a critical point which coincides with the *largest* possible value of p. The projection of the critical line on the (p, Y) plane is shown by a dotted line. We note that for a specified Y, there exists a maximum temperature beyond which no coexistence is possible. The projection of this

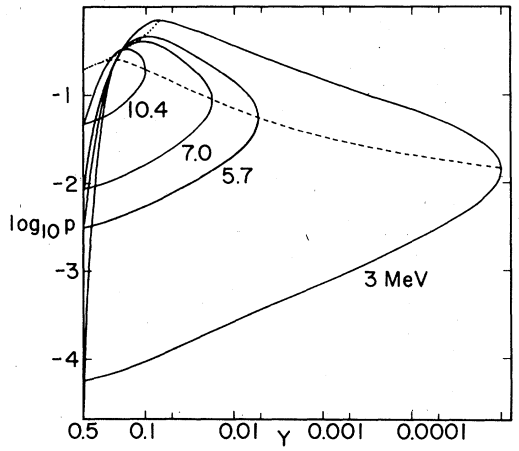

FIG. 6. Cuts of the phase-separation boundary surface orthogonal to T. The dotted line is the projection of the *critical* line, the dashed line the projection of the *maximum temperature* line. The *line of equal concentration* lies on the $Y = 0.5$ line.

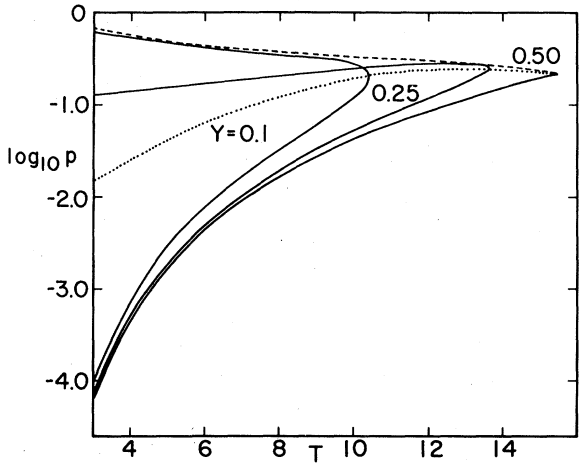

FIG. 8. Cuts of the phase separation boundary surface orthogonal to Y. The dashed line is the projection of the critical line, the dotted line the projection of the maximum temperature line.

line of maximum temperatures is shown as a dashed line. In general $T_{max} \neq T_{crit}$.

Interestingly our system also has a *line of equal concentrations* (LEC), namely a line for which $Y_a = Y_b$, but $\rho_a \neq \rho_b$. It is obvious that the LEC lies in the $Y = 0.5$ plane (see Fig. 5). The nature and existence of such a line can be seen from Fig. 9, which is the projection perpendicular to T of the coexistence surface in (p, T, ρ) space. Referring to the behavior of isobar (g) on Fig. 4, which loops back and cuts the $Y = 0.5$ line twice, we can imagine that there must be another isobar at somewhat lower pressure ($p = 0.044$ MeV/fm^3), for which the two intersection points on $Y = 0.5$ coincide, giving rise to a point of equal concentration. The FM thus has a cusplike behavior along the LEC, where the two sides of the FM are tangent to each other and to a plane parallel to the Y axis. It is easy to show (Ref. 23, Sec. 46) that $(dp/dY)_T = (dT/dY)_p = 0$ along the LEC (this does not show up in Figs. 5 and 6, because we have plotted $\log_{10} Y$). Two-phase coexistence is therefore possible when the isobars exhibit enough structure, i.e., from a pressure, p_{crit}, between curves c and e, where the isobar becomes multivalued down to a pressure $p_{eq,con}$, somewhat beyond curve g, where the loop of g has shrunk to a point and the isobar is again single valued.

This (p, T, ρ) coexistence surface, in contrast to the FM, is open toward low pressures. From Fig. 6 we infer that the lowest pressure points correspond to the LEC, which has the property of giving the largest density ratio between the coexisting phases.

According to the Gibbs phase rule the system can in principle have a *line* of three-phase coexistence, as well as a *point* of four-phase coexistence. The chemical potential isobars (Fig. 4) show that three-phase coexistence requires that a horizontal line (μ = constant) intersect a given isobar three times, with the additional constraint that all three intersection points be on a stable branch of the isobar. It appears unlikely that this can happen with the observed structure of the isobars, and, indeed, numerically we have not encountered a triple coexistence.

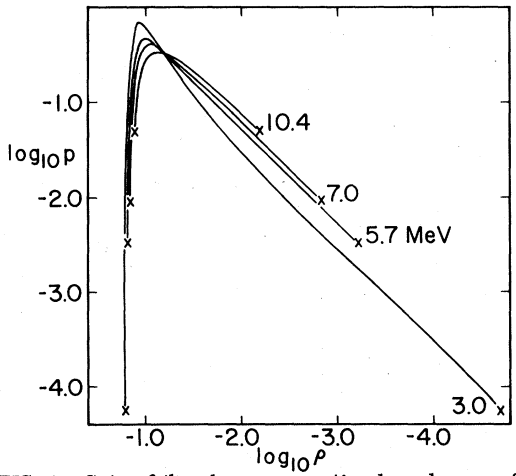

FIG. 9. Cuts of the phase separation boundary surface orthogonal to T, but for the density instead of Y.

Figure 6 shows that the critical pressure decreases with increasing temperature. This occurs because the critical point moves to lower density and the system is still very degenerate even at the critical temperature (see Fig. 9) and thence insensitive to temperature. The critical pressure also decreases with increasing Y (Fig. 6), achieving a minimum at $p^* \equiv p_{crit}(Y = 0.5) = 0.2$ MeV/fm^3 at a maximum critical temperature $T^* = 15.5$ MeV.

In Fig. 7 we exhibit cuts of the FM orthogonal to the p axis, for various values of p. It is worthwhile noting that for pressures lower than the critical pressure for symmetric matter, $p < p^*$, the isobars peak at $Y = 0.5$ on the LEC, whereas for $p > p^*$ they peak at their critical point, $T_{crit}(Y)$. This behavior is obvious from Fig. 5.

It is important to distinguish the *critical* temperature (the point on the FM, where the two coexisting phases are equal both in proton concentration and in density) from the *maximum* temperature (the highest temperature on the intersection of the FM with a Y = constant plane). This maximum temperature line has improperly been called critical (Ref. 19, e.g., Fig. 6, Ref. 13, and by Lamb *et al.*[11]); maximum and critical temperature with their textbook definitions coincide *only* for symmetric nuclear matter.

From Fig. 6 we can infer that the system undergoes a *retrograde condensation*. The part of the coexistence line running to the left of the critical point out to the point of equal concentration corresponds to the dense phase and the remainder to the light phase. Consider the behavior of a system undergoing an isothermal compression, say, at $T = 3$ MeV, with Y to the right of the critical point, say $Y = 0.01$. At a pressure of 2.6×10^{-4} MeV/fm^3, a dense phase of $Y = 0.46$ appears, increases in mass fraction until some maximum value, and then gradually fades away and disappears again at a pressure of 0.35 MeV/fm^3. To the left of the critical point, on the other hand, the behavior is normal with the dense phase gradually occupying the whole volume.

Finally Fig. 8 shows cuts perpendicular to the Y axis of the FM for several values of Y. For $Y = 0.5$ the two-phase coexistence region shrinks into a line, the LEC. Also shown is the projection of the LCP and the projection of the line of

maximum temperature. All three lines terminate at the same point, which is thus the critical point for symmetric matter, and also the highest temperature at which any phase coexistence is possible. With decreasing proton concentration Y the phase-coexistence domain shrinks at lower temperature, until it becomes a point at zero temperature, at some value of $Y>0$. The pure neutron gas at zero temperature is stable against breakup into two phases; indeed, the zero temperature isotherm, $p(\rho)$, is a monotonically increasing function. The FM therefore does not touch the $Y=0$ plane and a pure-phase coexistence line does not exist.

For a given average $Y=0.5$, we infer from Fig. 2 that for a specified temperature and pressure, say, $p<p_{\text{vaporization}}$, the system can exist in a stable mono-phase state, represented by the point on the left-hand side of the $p(\rho, T, Y)$ curve, as well as in the metastable mono-phase state, corresponding to the point on the right-hand side. In addition there exists a metastable two-phase state with equal densities, $\rho_a=\rho_b$, and mass fractions ($\xi=0.5$), but with unequal, symmetric proton concentrations, $Y_b=1-Y_a$. The existence of this curious state can be inferred[25] from the symmetric extension of the chemical potential isobars (Fig. 4) from $Y=0.5$ to 1.0. It is clearly a result of the assumption of the isobaric charge symmetry of nuclear forces.

At this stage it may be worthwhile to point out that the solution to the phase equilibrium equations is not unique, which creates a numerical nightmare. For example it is easy to see from Fig. 4 that in addition to the exhibited rectangle on isobar (f) there must exist two other rectangles on the *same* isobar. Both of these, however, have one phase which lies on an unstable branch of the isobar and hence must be discarded. Especially, slightly below the critical pressure, it is essentially impossible to find a solution numerically and we have accordingly interpolated the curves in this narrow region.

It is interesting to study the behavior of the system as a function of the *average* extensive variables, ρ and Y. This is a more useful way of looking at such matter undergoing compression or heating, since we normally specify T, ρ, Y and are interested in the resulting pressure and phase configuration. Denoting by ξ the mass fraction of phase (a) we then have the relations

$$Y=\xi Y_a+(1-\xi)Y_b, \tag{9}$$

$$\frac{1}{\rho}=\frac{\xi}{\rho_a}+(1-\xi)\frac{1}{\rho_b}. \tag{10}$$

The curve labeled ρ_1 in Fig. 10 represents, for a given average $Y=0.1$, the stable solution of the coexistence Eqs. (6)–(8) and of Eqs. (9) and (10) with $\xi=1$. It thus delineates from above the two-phase coexistence region. The peak temperature ($T_{\max}=10.4$ MeV for $Y=0.1$, see Fig. 6) falls on the line of maximum temperature as defined above. Also shown on the same graph is the density (curve ρ_2) of the incipient phase [i.e., phase (b) with $\xi=0$]. That the peak of curve ρ_1 is *not* a critical point is thus obvious since $\rho_2\neq\rho_1$ and $Y_2\neq Y_1=0.1$. The crossing point γ of curves ρ_1 and ρ_2, on the other hand, clearly corresponds to the *critical* point ($T_{\text{crit}}=5.7$ MeV for $Y=0.1$, see Fig. 6). It is worth mentioning that the well-known lever rule[24] which was applicable to Figs. 5 to 8 is no longer valid in this figure [we now specify the *average extensive* variable ρ in addition to T, but no longer specify the (intensive) pressure]. The instability boundary (dashed line) for $Y=0.1$ is seen to fall inside the coexistence boundary and touches the latter at the critical point as it must. The region between these two boundaries corresponds to *metastable* single phase states.

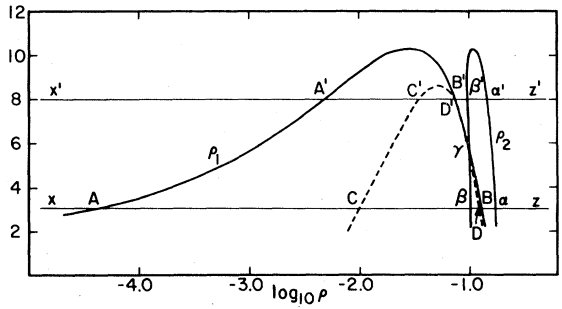

FIG. 10. Phase diagram for an average $Y=0.1$. The thick line labeled ρ_1 is the boundary of phase separation. The line ρ_2 denotes the density of the incipient phase. The instability line (dotted) for the single phase touches the phase separation line ρ_1 at the critical point γ.

The existence of a critical point gives rise to an already mentioned interesting behavior in an isothermal compression, behavior which differs depending on whether the temperature is greater or smaller than $T_{\text{crit}}=5.7$ MeV (point γ). During an isothermal compression below T_{crit} (line xz in Fig. 10), at point A the system undergoes a phase separation (although it could stay metastable up to point C, the instability boundary). The incipient phase is denoted by α and has a *higher* density. At point B the system goes back into a single phase. (In a decompression this single phase could metastably last from B to D.) At point B the disappearing phase has a density β which is *lower* than that of the principal phase. The behavior of the system throughout the two-phase region is reported in Fig. 11 as a function of the average

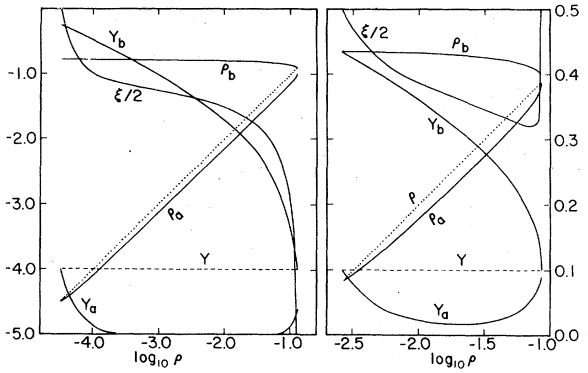

FIG. 11. Variation of the properties of the two coexisting phases a and b and the mass fraction of phase a throughout an isothermal compression as a function of the average density for $Y=0.1$. (1) for $T=3$ MeV$<T_{crit}$ (2) for $T=7$ MeV$>T_{crit}$. The left-hand scale refers to the (decimal) logarithm of the densities and the right-hand scale to the proton fractions and mass fractions. The dotted line corresponds to the average density ρ.

density ρ. In particular from Fig. 11(a) which corresponds to a temperature $T<T_{crit}$ we note that the mass fraction ξ varies from 1 to 0 indicating that the second (denser) phase (b) gradually takes over completely from the first phase (a). Phases (a) and (b) vary smoothly with the average density as Fig. 11 shows (Gibb's level rule no longer works as pointed out above).

Above the critical temperature (crossing point, labeled γ in Fig. 10) a qualitatively different behavior sets in. At A' a new *denser* phase α' appears as before, but at the other side of the two-phase region, point B', the disappearing phase now also is *denser* than the principal phase. The curve for ξ in Fig. 11(b) indicates that the mass fraction of the *denser* phase, which appears at A', never exceeds some maximum value, after which it fades away again. The critical temperature, at which the disappearing and the principal phases are the same, separates the normal and retrograde behavior. This retrograde behavior was overlooked in the description of Ref. 19.

Figure 12 shows the behavior of ξ as a function of the average density ρ for several temperatures. At the critical temperature, ξ is undefined since the coexisting phases are identical. Above T_{crit} the appearance of the retrograde behavior clearly stands out.

Finally in Fig. 13 we show the coexistence boundaries (similar to Fig. 10) for several values of Y. Below a certain value of Y (approximately $Y=0.05$, see Figs. 5 and 6) there no longer exists a critical point, so that the ρ_1 and ρ_2 curves, analogous to Fig. 13, no longer intersect (no γ point). A point of maximum temperature nevertheless continues to exist.

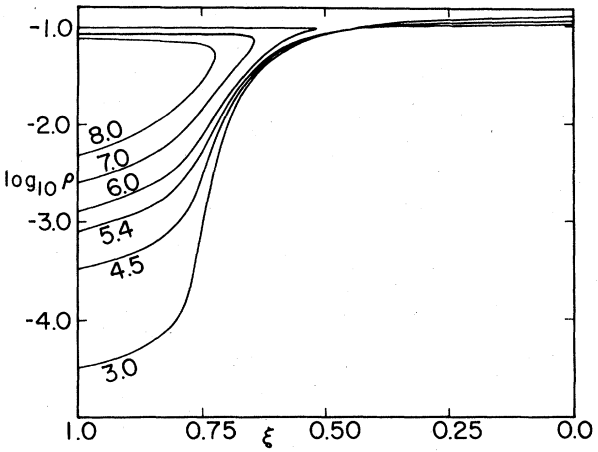

FIG. 12. Behavior of the mass fraction ξ of phase a as a function of average density. Temperature ranges from 3 to 8 MeV.

For the purpose of comparison we also show the coexistence boundary[26] of Ref. 19 for $Y=0.5$; their maximum and critical (because $Y=0.5$) temperature ($T_{max}=20.5$ MeV) is considerably higher than ours ($T_{max}=15.5$ MeV), but the qualitative behavior is very similar. In particular the energy functional used in Refs. 11 and 19 also gives rise to a crossing point[26] and hence indicates the presence of a critical point. We have also computed the maximum critical temperature for another energy functional[27] and found it to be $T_{max} \simeq 16.2$ MeV. A comparison of these three maximal temperatures gives us a measure of the sensitivity of the results to the nuclear interaction energy.

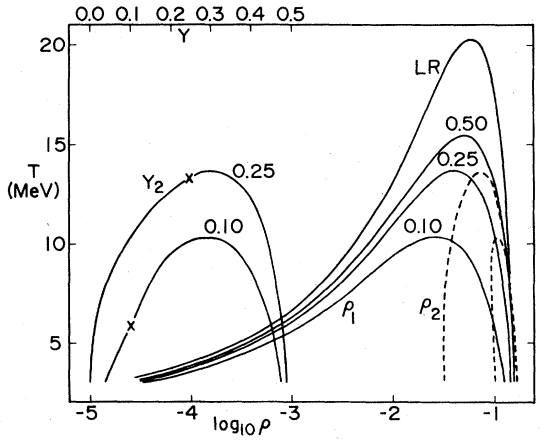

FIG. 13. Phase diagram (same as Fig. 10) in terms of average ρ for $Y=0.1$, 0.25, and 0.50. In addition is shown Y_2. Note that the right-hand branch of ρ_2 and the right-hand branch of Y_2 correspond to the left-hand branch of ρ_1. Also shown for comparison is the $Y=0.5$ curve for the nuclear interaction energy of Refs. 11 and 19 (LR).

Also shown in the same graph is the proton concentration, Y_2, of the incipient phase. Again the left (right) branches of the Y_2 and ρ_2 curves correspond to the right (left) branch of the ρ_1 curve.

Finally, we can discuss the actual equation of state for our system. In Fig. 2 which refers to symmetric matter ($Y=0.5$), the dashed line indicates the phase separation line. Upon compression along a given isotherm the system follows the solid line from the origin until the point of intersection with the phase separation line, then runs across horizontally until it meets again the single phase (solid) line which it then follows. Metastability is possible at positive pressures between the phase separation line and the instability line. The fact that the traversal of the coexistence region occurs at constant pressure $p_{\text{vaporization}}$ can be inferred from Fig. 8 and is due to the existence of the line of equal concentrations. For a general Y, e.g., $Y=0.1$ (Fig. 3) the equation of state is therefore more complicated. At both points of phase separation the pressure deviates abruptly from the single phase pressure of same density. A metastable region also exists in the vicinity of these points (dashed line) separated by an unstable excluded region (dotted line). The retrograde behavior discussed above does not show up at all in the equation of state $p(\rho, T)$, nor does the existence of a critical point. Their presence is only reflected at the more detailed level of description of the consistuency of matter.

We have not bothered to include the effects of leptons in the equation of state of bulk matter at this stage, although one could this way get a reasonable approximation to the actual equation of state. We stress that if the phase coexistence were neglected, however, such an equation of state would be grossly inadequate as can be seen from Figs. 2 and 3.

IV. CONCLUSIONS

The thermodynamic properties of dense, hot nuclear matter are those expected of a binary liquid-vapor mixture. It has special features, which not all such binary systems need to have, namely that there exists a line of critical points as well as a line of equal concentrations. There are therefore conditions under which the phenomenon of retrograde condensation exists.

The existence of a line of critical points implies the existence of a line of maximum temperatures. It is clear from Fig. 6 that along the phase-separation boundary (ρ_1 curve in Fig. 10) at fixed Y the maximum temperature must be larger than the critical temperature. Coexistence of more than two phases, although possible in principle, does not exist for nuclear matter.

Whether the retrograde features survive when Coulomb and surface effects are included is not clear; if they do one would expect the large fluctuations in nuclear size distributions to occur near the critical point and not near the maximum temperature. In the approximation of representing the distribution of nuclei by a single typical nucleus, the lines of constant atomic number (see, e.g., Ref. 11) would thus tend to converge on the critical point and not the point of maximum temperature.

The extension of this work to include surface and Coulomb effects is in progress. Our approach is based on a warm nuclear Thomas-Fermi model.[13,8] It has been shown[20] that our formalism is capable of adequately reproducing the average excitation spectrum and hence the specific heat of nuclei. An accurate knowledge of the sizes of nuclei in hot matter has a bearing on the fate of the collapsing cores, since neutrino opacities are sensitive to the atomic number.

ACKNOWLEDGMENTS

It is a pleasure to acknowledge fruitful discussions with Gordon Baym, Don Lamb, and Jim Lattimer in the stimulating atmosphere of the Aspen Center for Physics, as well as with John O'Connell at the University of Florida. One of us (J.R.B.) thanks Jean-Pierre Hansen for his hospitality at the Université de Paris VI, where this work was started. The other of us (M.B.) thanks Roland Lombard for his hospitality at the IPN d'Orsay. We also gratefully acknowledge the support of the National Science Foundation (Grant Nos. AST77-17572 and AST79-20024) and the generous computer support of the Northeast Regional Data Center and of the Bureau de Calcul de l'IPN d'Orsay.

[1] S. A. Colgate and R. H. White, Astrophys. J. 143, 626 (1966).
[2] J. R. Wilson, *Sources of Gravitational Radiation*, edited by L. L. Smarr (Cambridge University Press, Cambridge, 1979).
[3] K. Van Riper and W. D. Arnett, Astrophys. J. Lett. 225, L129 (1978).
[4] M. Livio, J. R. Buchler, and S. A. Colgate, Astrophys. J. Lett. (to be published).
[5] R. I. Epstein, Mon. Not. R. Astron. Soc. 188, 305 (1979).

[6]S. A. Colgate and A. Petschek, Astrophys. J. Lett. (in press).
[7]S. W. Bruenn, J. R. Buchler, and M. Livio, Astrophys. J. Lett. 234, L73 (1980).
[8]Z. K. Barkat, J. R. Buchler, and L. Ingber, Astrophys. J. 176, 723 (1972).
[9]J. W. Negele and D. Vautherin, Nucl. Phys. A207, 298 (1973).
[10]G. Baym, H. A. Bethe, and C. J. Pethick, Nucl. Phys. A175, 225 (1971).
[11]D. W. Lamb, J. M. Lattimer, C. J. Pethick, and D. G. Ravenhall, Phys. Rev. Lett. 41, 1623 (1978).
[12]H. A. Bethe, G. E. Brown, J. Applegate, and J. M. Latimer, Nucl. Phys. A324, 487 (1979).
[13]J. R. Buchler and M. Barranco, Phys. (Paris) Colloq. C2, Supplement No. 3, Tome 41 (1980).
[14]W. A. Küpper, G. Wegmann, and E. R. Hilf, Ann. Phys. (N.Y.) 88, 454 (1974).
[15]J. R. Buchler and S. A. Coon in *Quantum Statistics and the Many Body Problem*, edited by S. B. Trickey, W. P. Kink, and J. W. Duffy (Plenum, N. Y., 1975), and Astrophys. J. 212, 807 (1977).
[16]M. F. ElEid and E. R. Hilf, Astron. Astrophys. 57, 243 (1974).
[17]J. R. Buchler and B. Datta, Phys. Rev. C 19, 494 (1979).
[18]M. Kiguchi, Progr. Theor. Phys. 57, 1572 (1977).
[19]J. M. Lattimer and D. G. Ravenhall, Astrophys. J. 223, 314 (1978).
[20]J. R. Buchler and R. I. Epstein, Astrophys. J. Lett. 235, L91 (1980).
[21]R. J. Lombard, Ann. Phys. (N.Y.) 77, 380 (1973).
[22]J. R. Buchler and L. Ingber, Astrophys. J. A170, 1 (1971).
[23]R. Haase, *Thermodynamik der Mischphasen* (Springer, Berlin, 1956).
[24]L. Landau and E. Lifshitz, *Physique Statistique* (Editions Mir, Moscow, 1967).
[25]J. R. Buchler and J. M. Lattimer (unpublished).
[26]J. M. Lattimer, private communication.
[27]H. Krivine, J. Treiner, and O. Bohigas, Orsay Report No. IPNO/TH-79-29 (1979), Nucl. Phys. A (in press).